Phase Transitions, 1986, Vol. 8, pp. 35–57
0141-1594/86/0801-0035$18.50/0
© 1986 Gordon and Breach Science Publishers
Printed in the United Kingdom

Structure and Phase Transitions of Graphite Intercalated with Bromine

D. D. L. CHUNG†

Department of Metallurgical Engineering and Materials Science, Carnegie-Mellon University, Pittsburgh, Pennsylvania 15213, U.S.A.

(*Received June 19, 1986*)

This paper is a review of the structure and phase transitions of graphite-bromine intercalation compounds. Emphasis is given to the room-temperature commensurate phase, the room-temperature incommensurate phase and the high-temperature incommensurate phase, together with the associated intralayer commensurate-incommensurate transition (332–350 K, depending on the stage), incommensurate–commensurate transition (319 K) and melting transition (374 K). Other transitions are the interlayer order-order transition (297 K) and the interlayer disorder–order transition (277 K). Of fundamental importance are the determination of the two-dimensional structure of the commensurate phase and the successful use of domain wall models to elucidate incommensurate phases. The dependence of the structure and phase transitions on stage and sample preparation conditions is also summarized.

KEYWORDS graphite, intercalation, bromine, structure, phase transition.

INTRODUCTION

Graphite intercalation compounds have received much attention during the last ten years because of their unusual structure, high electrical conductivity, electrochemical behavior and catalytic properties. Dozens of chemicals (known as intercalates) have been shown to intercalate graphite. They include the alkali metals (such as potassium), the

---

† Partly supported by the ALCOA Foundation.

halogens (such as bromine), acids (such as nitric acid) and metal halides (such as ferric chloride). An intercalate may act as an electron donor or an electron acceptor, thereby doping the graphite.

An intercalation compound of graphite is made up of carbon and intercalate layers which are stacked periodically, forming a superlattice along the c-direction. The number of carbon layers between nearest intercalate layers is known as the stage of the compound. This aspect of the structure of graphite intercalation compounds is well-known, but the in-plane structure is not known for most compounds. By the in-plane structure, we refer to the in-plane unit cell as well as the locations of the atoms within the unit cell. For many years, the only compounds for which the in-plane structure had been established were the stage-1 graphite-alkali metals (donor compounds), which exhibit rather simple in-plane crystal structures (Rüdorff and Schulze, 1954). Such simplicity does not apply to other compounds, as evident by their more complex in-plane diffraction patterns.

An attractive property of graphite intercalation compounds is the high electrical conductivity in the in-plane direction. The highest conductivities in these materials are found in acceptor compounds, e.g. $SbCl_5$, AsF_5, ICl, etc. However, that these intercalates are not pure elements complicates their structure. Bromine is practically the only elemental acceptor intercalate, and so it is attractive for a fundamental study.

The bromination of graphite fibers has recently attracted technological interest because it produces highly conductive fibers that are stable in vacuum, water and heat (Gaier and Jaworske, 1985). However, the actual occurrence of intercalation in these fibers was assumed without any firm evidence for intercalation.

Much progress has recently been made in studying the structure and phase transitions of graphite-bromine. This paper provides a review on this subject.

OVERVIEW

Synchrotron single-crystal x-ray diffraction results have established the in-plane structure of the room-temperature commensurate (β) phase of stage-2 graphite-bromine (Ghosh and Chung, 1982; Ghosh and Chung, 1983a; Ghosh and Chung, 1983b). The solution of this structure has

TABLE I

Phase transition temperatures of graphite-bromine

Transition Type upon heating	Transition Temperature (K)				
	Stage 2		Stage 3	Stage 4	Type C (desorbed from Type A)
	Type B	Type A			
α–L				373	374
β–α	332	333	337	342	350
α'–β				277	
γ–β	319				
δ–γ	297				
ε–δ	277				
η–β		240			226

L: liquid phase
β, ε: commensurate solid phases
α, α', γ, δ: incommensurate solid phases; α and α' are similar.
η: other solid phase

opened up new ground for understanding the behavior of this phase, for which much information is available in the literature. Furthermore, it sheds light on the structure of other graphite-bromine phases, such as the room-temperature incommensurate (γ) phase (Ghosh and Chung, 1983c, 1983d; Moret, Comes, Furdin, Fuzellier and Rousseaux, 1983; Aberkane, Rousseaux, Samuelson and Moret, 1986), the high-temperature incommensurate (α) phase (Bardhan, Wu and Chung, 1980; Kortan, Erbil, Birgeneau and Dresselhaus, 1982), and the low-temperature incommensurate (α') phase (Kortan, Birgeneau and Dresselhaus, 1986). For these incommensurate phases domain wall models have been found to agree with the experimental data, but the in-plane structures of these phases have not been fully established (Ghosh and Chung, 1983d; Kortan, Erbil, Birgeneau and Dresselhaus, 1982). Other than the β, γ, α and α' phases, three other phases (δ, ε, η) have been observed at lower temperatures, though their structures remain to be determined. Differential scanning calorimetry (DSC) and x-ray diffraction showed that the δ–γ phase transition occurs at 297 K (Bardhan, Wu and Chung, 1980; Culik and Chung, 1979; Moret, Comes, Furdin, Fuzellier and Rousseaux, 1983; Aberkane, Moret, Comes, Furdin and Herold, 1985) and the ε–δ phase transition occurs at 277 K (Bardhan

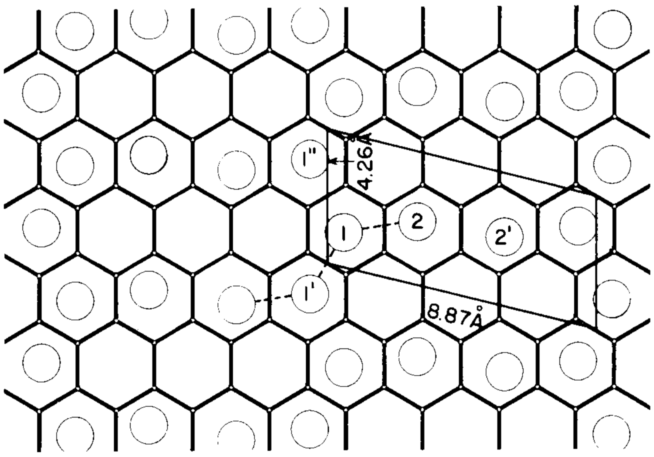

FIGURE 1 Two-dimensional structure of Type A graphite-bromine at room temperature. The unit cell is indicated by the parallelogram. The interatomic distances are Br1–Br1′: 2.25 Å; Br1–Br2: 2.38 Å; Br1–Br1″: 2.55 Å; Br2–Br2′: 2.86 Å. (After Ghosh and Chung, 1983b).

et al., 1980; Culik and Chung, 1979; Aberkane, Moret, Comes, Furdin and Herold, 1985; Culik and Chung, 1984). Moreover, x-ray diffraction (Bardhan *et al.*, 1980) showed that the η–ε phase transition occurs at 226 K and that this transition corresponds to the change from streaks to spots in the electron diffraction pattern (Bardhan *et al.*, 1980; Eeles and Turnbull, 1965). The various observed phase transition temperatures are summarized in Table I, where Type B refers to stage 2 prepared in liquid bromine at room temperature, and Type C refers to an indefinite stage(s) obtained by deintercalation (or desorption) of Type A.

The following sections review the phases one by one.

PHASE β

Phase β refers to the room temperature commensurate phase. It is the most commonly seen phase of graphite-bromine, exhibiting a three-fold twinned monoclinic unit cell ($a = 8.87$ Å, $b = 4.26$ Å, $\gamma = 103.9°$) (Ghosh and Chung, 1982, 1983a). Below 325 K, there is partial correlation between the nearest intercalate layers, as indicated by a 30%

sinusoidal modulation of the Bragg rods along the c^*-direction; above 325 K, the layers are completely uncorrelated (Erbil, Kortan, Birgeneau and Dresselhaus, 1983a; Erbil, Kortan, Birgeneau and Dresselhaus, 1983b).

The in-plane structure of phase β has been solved for Type A (stage-2 C_7Br) (Ghosh and Chung, 1983b) and Type C (overall stoichiometry of $C_{35}Br$) (Ghosh and Chung, 1983e) at room temperature. Although the diffraction patterns of Types A and C consist of diffraction peaks in the same positions, there are differences in the relative intensities of the peaks. As a result, Type A and Type C have different in-plane structures, though the in-plane unit cells are the same. For Type A, the two atoms in the asymmetric unit (Br1, Br2) have the same occupancy factor whereas, for Type C, the occupancy factor of Br1 is twice of that of Br2. For Type A (Figure 1), the nearest neighbor distances between the bromine atoms are 2.25 (±0.05), 2.55 (±0.05), 2.38 (±0.05) and 2.86 (±0.06) Å (Ghosh and Chung, 1983b), whereas they are, for Type C (Figure 2), 2.29 (±0.06), 2.43 (±0.06), 2.10 (±0.07) and 3.48 (±0.07) Å (Ghosh and Chung, 1983e). The first two distances are close for Types A and C. The third distance is smaller for Type C than Type A; the value for Type C is even smaller than the intramolecular distance

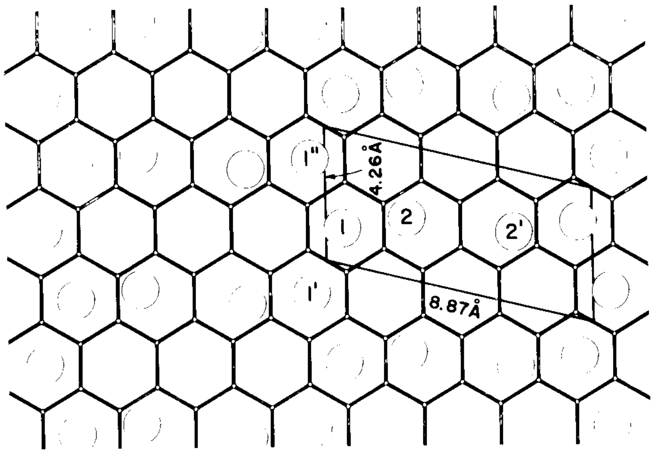

FIGURE 2 Two-dimensional structure of Type C graphite-bromine at room temperature. The unit cell is indicated by the parallelogram. The interatomic distances are Br1–Br1′: 2.29 Å; Br1–Br2: 2.10 Å; Br1–Br1″: 2.43 Å; Br2–Br2′: 3.48 Å. (After Ghosh and Chung, 1983e).

(2.28 Å) in solid bromine. The fourth distance is considerably larger for Type C than for Type A; the value for Type C is even larger than the smallest intermolecular distance of 3.34 Å in solid bromine. Because the distance between Br1 and Br2 in Type C is less than the intramolecular distance in solid bromine and because in Type C Br1 has an occupancy factor that is twice of that of Br2, a phase with an in-plane intercalate density which is half of that of Type A (stage-2 C_7Br) must be present in Type C (Ghosh and Chung, 1983e). This low in-plane intercalate density is consistent with the recent report of Furdin (1983) that the desorption of Stage-2 C_8Br resulted in stage-2 $C_{14}Br$, stage-3 $C_{21}Br$ and stage-4 $C_{28}Br$. Stage-2 $C_{14}Br$ has the same unit cell as phase β (Moret, Rousseaux, Furdin and Herold, 1983). Thus, there are two or more room temperature commensurate phases, which are referred to as phase β_1 (in Type A) and phase β_2 (in Type C). The term "phase β" refers to phase β_1 and/or phase β_2.

Let us consider the chemical bonding between the bromine atoms in Type A, which consists of only one phase, i.e. phase β_1. The largest interatomic distance, 2.86 Å, is approximately along the direction perpendicular to the *b*-axis (Ghosh and Chung, 1983b). Thus, approximately, the bromine atoms are distributed in zig-zag polymeric chains along the *b*-axis and the chains are spaced 8.61 Å apart (Figure 1). The cluster of four atoms, shown connected in Figure 1 by dashed lines, forms one unit of a chain; the units are linked to each other through the 2.55 Å distance (Ghosh and Chung, 1983b). The similarity in Br–Br distances with those of Br_3^-, Br_4^{2-} and Br_5^- (Figure 3) suggests that the

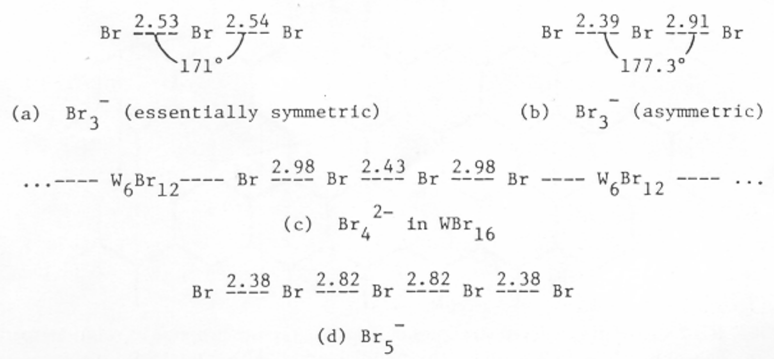

FIGURE 3 Polybromide anions. Bond distances are in Å. (After Ghosh and Chung, 1983b).

interacting Br_4^{x-} units in graphite-bromine have a character which resembles Br_3^-, Br_4^{2-}, Br_5^- or other polybromide anions. The possible hypervalency (trivalency) for bromine (Reese, 1983) also supports the chemical plausibility of the structure.

The Raman-active Br-Br stretching modes for the asymmetric Br_3^- occur at 249 and 135 cm^{-1} in $PBr_4^+Br_3^-$ (Gabes and Berding, 1971). Those for Br_5^- occur at 245 cm^{-1} (intense) and 157 cm^{-1} (weak) in brominated nickel and palladium bis (diphenylglyoximates) (Kalina, Lyding, Ratajack, Kannewurf and Marks, 1980). The 249 cm^{-1} frequency of Br_3^- and the 245 cm^{-1} frequency of Br_3^- and the 245 cm^{-1} frequency of Br_5^- are close to the main intercalate Raman mode frequency of 242 cm^{-1} in graphite-bromine (Song, Chung, Eklund and Dresselhaus, 1976; Eklund, Kambe, Dresselhaus and Dresselhaus, 1978). In contrast, the vibrational frequency of the free Br_2 molecule is 323 cm^{-1} (Herzberg, 1945) and that of solid bromine is 300 cm^{-1} (Cahill and Leroi, 1969). Furthermore, the 157 cm^{-1} frequency of Br_5^- is close to the weak intercalate Raman mode frequency of 152 cm^{-1} in graphite-bromine (Song *et al.*, 1976; Eklund *et al.*, 1978). Therefore, Raman scattering data support the long-chain polymeric bromine structure (Ghosh and Chung, 1983b) rather than the molecular Br_2 structure (Song *et al.*, 1976; Eklund *et al.*, 1978) in graphite-bromine. The long-chain polymeric bromine structure is also supported by calculation of the Raman frequencies in graphite-bromine using a Born-von Kármán lattice dynamical model (Al-Jishi and Dresselhaus, 1983). This calculation showed that Br atom displacement along the chain corresponded to a B_{1g} mode, which occurred at 246 cm^{-1} (Al-Jishi and Dresselhaus, 1983). A chain model is furthermore supported by the phonon spectrum determined by inelastic neutron scattering in graphite-bromine (Simon, Batallan, Rosenman, Lauter and Furdin, 1983; Batallan, Rosenman, Simon, Lauter and Furdin, 1983; Batallan, Rosenman and Simon, 1983; Batallan, Rosenman, Simon, Furdin and Lauter, 1981). On the other hand, EXAFS results suggest a single Br-Br distance (Feldman, Skelton, Dominguez, Elam, Qadri and Lytle, 1984; Feldman, Elam, Ehrlich, Skelton, Dominguez, Qadri, Chung and Lytle, 1983; Feldman, Elam, Ehrlich, Skelton, Dominguez, Chung and Lytle, 1986).

Other than the bromine structure, the carbon structure and the in-plane relationship of the bromine layer with respect to the carbon layers can also be obtained from the x-ray diffraction results. The in-plane relationship of the bromine atoms with respect to the carbon atoms has been determined, as shown in Figure 1 for phase β_1 (Ghosh and Chung, 1983b). Because of the possible contribution of free graphite regions to the diffraction data, the intensities of the six *hk* graphitic reflections need to be measured away from the (*hki*0) graphite plane, at hypothetical *hk*1 ($l = 1$) positions.

This had been performed on phase β_1 using sealed-tube x-rays, as shown in Figure 4 (Ghosh and Chung, 1983b). However, the resolution in the resulting difference electron density map was insufficient to give the exact carbon-carbon bond lengths.

The difference electron density map (Figure 4) obtained with sealed-tube x-rays exhibits a single unique position of the carbon plane, indicating A-A stacking of the two carbon planes adjacent to a bromine plane, as well as the positions of the bromine atoms with respect to the carbon atoms (Ghosh and Chung, 1983b). Further support for the A-A stacking was obtained from structure factor calculations, which yielded

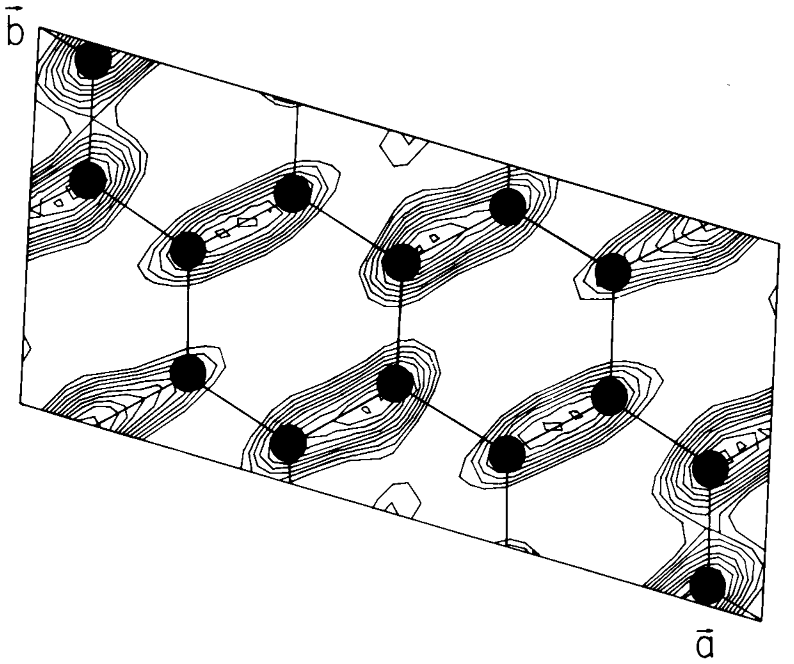

FIGURE 4 Difference electron density map calculated with all reflections, revealing the graphite structure in two-dimensional projection. (After Ghosh and Chung, 1983b).

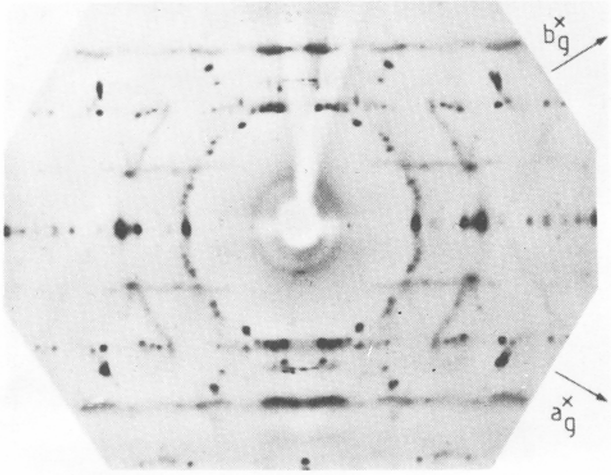

FIGURE 5 (*hk*0) precession photograph of C_8Br at room temperature. (After Moret, Rousseaux, Furdin and Herold, 1983).

a lower *R* factor for A–A stacking than for A–B stacking (Ghosh and Chung, 1983b).

The structure presented above for phase β does not account for the streaks, which occur at incommensurate positions and are due to a minor incommensurate phase (Ghosh and Chung, 1983a; Moret, Rousseaux, Furdin and Herold, 1983). These streaks are at h, k ($k \neq 0$) positions parallel to the a^*-direction, suggesting that the bromine chains are periodically spaced along the *a*-direction, while the atom-to-atom correlation along the *b*-direction among the chains is limited (Ghosh and Chung, 1983a). The streaks occur at 0.488 a_g^* [i.e., $(0.5 - 0.012)a_g^*$] and $0.762a_g^*$ [i.e., $(0.75 + 0.012)a_g^*$] (Moret, Rousseaux, Furdin and Herold, 1983). These streaks are weak compared with the commensurate diffraction spots. However, in phase γ (in stage 2, Type B), these streaks became strong (Ghosh and Chung, 1983c).

PHASE γ

Phase γ refers to the room-temperature incommensurate phase. It had been observed in stage-2 graphite-bromine prepared in bromine liquid, i.e. Type B (Ghosh and Chung, 1983c, 1983d). This phase was also

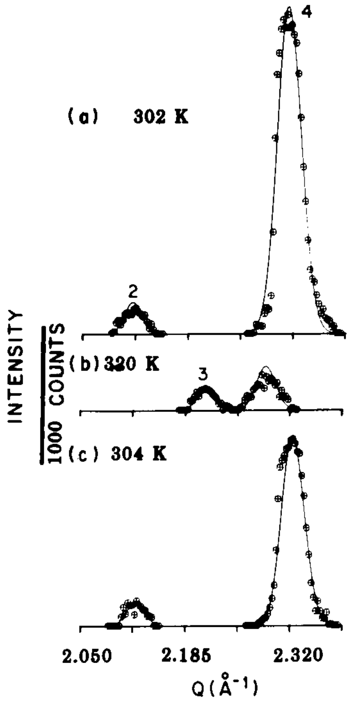

FIGURE 6 Scan of intensity vs. Q for Type B graphite-bromine along a^* in the vicinity of 3,0 of the commensurate phase. The peaks are labelled as 2, 3 and 4. (After Ghosh and Chung, 1983d).

observed in a saturated stage-2 compound (of nominal composition C_8Br) prepared by using the two-zone furnace technique (Moret, Comes, Furdin, Fuzellier and Rousseaux, 1983).

Figure 1 of Ghosh and Chung (1983c) and Figure 5 of Moret, Comes, Furdin, Fuzellier and Rousseaux (1983) show the in-plane diffraction pattern of phase γ. The latter was taken with rotating-anode x-rays and was clearer, and so it is shown in Figure 5. Shown in Figure 6(a) and Figure 7(a) are synchrotron x-ray diffraction intensity scans along the a^*-direction, which is the most incommensurate direction of the lattice (Ghosh and Chung, 1983d).

In Phase γ, the strongest in-plane superlattice reflection (i.e., the 3,0 reflection at Q_c) in phase β was replaced by incommensurate peaks at Q_c $(1 - 0.033)$ and Q_c $(1 + 0.058)$ (Figure 6(a)) (Ghosh and Chung,

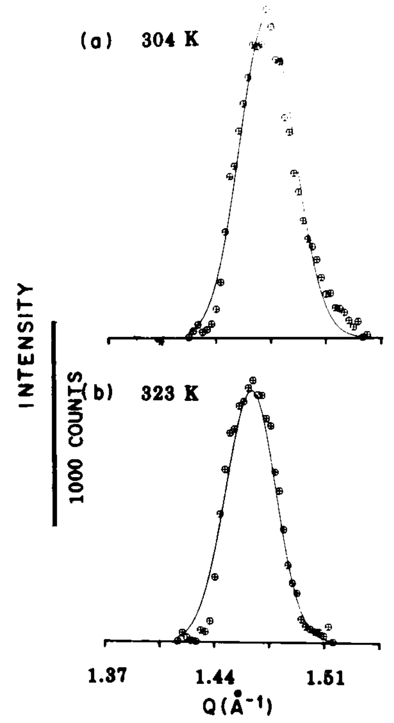

FIGURE 7 Scan of intensity vs. *Q* for Type B graphite-bromine along *a** in the vicinity of 2,0 of the commensurate phase, showing Peak 1. (After Ghosh and Chung, 1983d).

1983d). Moreover, in Phase γ, the 2,0 reflection of Phase β appeared at a slightly higher *Q* value (Figure 7(a)). In addition, diffuse lines weakly present in phase β developed strongly in phase γ at *h*, *k* ($k \neq 0$) positions parallel to the *a**-direction. These observations suggested that the bromine chains along the b-direction in phase γ are periodically spaced, while the atom-to-atom correlation along the *b*-direction among the chains is limited (Ghosh and Chung, 1983c, 1983d). The situation is thus quasi one-dimensional.

Upon heating Type B, phase γ transforms reversibly to Phase β at 319 ± 1 K (Ghosh and Chung, 1983c, 1983d). This is termed an incommensurate-commensurate (γ-β) transition. Upon further heating Type B, Phase β transforms reversibly to Phase α at 332 K (Ghosh and

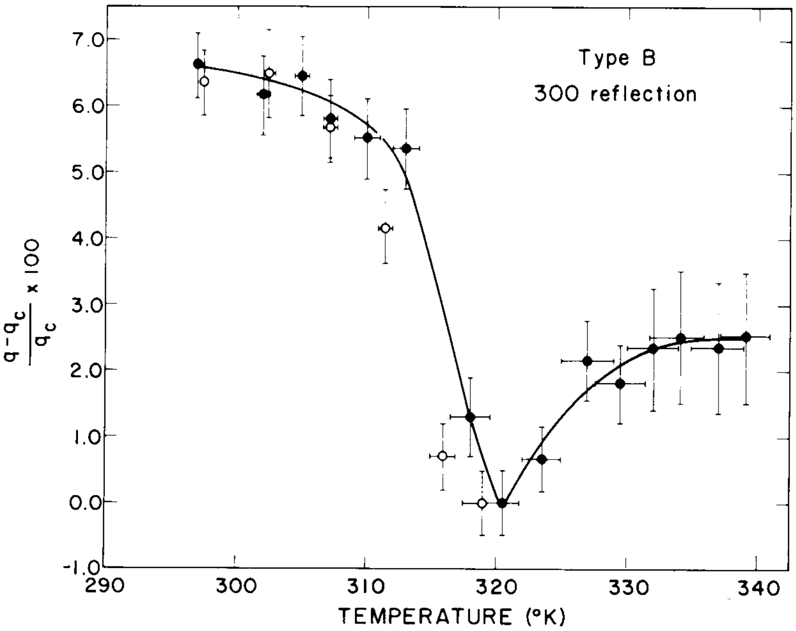

FIGURE 8 Misfit parameter vs. temperature for Type B graphite-bromine. The smooth curve is an approximate guide to the course of change of the parameter. ●: during heating; ○: during cooling. (After Ghosh and Chung, 1983c).

Chung, 1983c); this is the commensurate-incommensurate (β-α) transition which was also observed in stage 2 (Type A) (Ghosh and Chung, 1983c), stage 3 (Ghosh and Chung, 1983c), stage 4 (Ghosh and Chung, 1983c; Kortan *et al.*, 1982; Erbil *et al.*, 1983a; Erbil *et al.*, 1983b) and Type C (Ghosh and Chung, 1983c). Figure 8 shows a plot of the misfit parameter vs. temperature for Type B over a temperature range which covers both the γ-β and β-α transitions (Ghosh and Chung, 1983c). Phase γ (the low-temperature incommensurate phase) is much more incommensurate than Phase α (the high-temperature incommensurate phase). The γ-β transition is characterized by the disappearance of the incommensurate peaks at $Q_c(1 - 0.033)$ and $Q_c(1 + 0.058)$ and the appearance of the commensurate peak at Q_c (Ghosh and Chung, 1983d), in contrast to the slight shifts of the peaks in the β-α transition (Bardhan *et al.*, 1980; Kortan *et al.*, 1982).

A one-dimensional domain wall model has been used to explain the strongest diffraction peaks, which are along the a^*-direction (Ghosh and Chung, 1983d). In this model, the domains have Marti and Thorel (1977) type unregistry, and the interchain distance is taken as 8.133 Å, the domain wall thickness as 5.32 Å, and the domain wall spacing as 29.72 ± 0.03 Å. On the other hand, the whole ($hk0$) diffraction pattern can be explained by using an incommensurate unit cell ($a = 4.36$ Å, $b = 8.63$ Å, $\gamma = 99.45^\circ$, a^* along [110]) modulated by the graphite (Aberkane *et al.*, 1986).

Scanning along the c^*-direction showed reversible shifts in the prominent $00l$ peak positions at the γ–β transition (Ghosh and Chung, 1985). The shifts indicate a change of the sandwich thickness from 10.40 ± 0.01 Å for phase γ to 10.22 ± 0.01 Å for Phase β. This suggests that the bromine atoms between two carbon layers in the incommensurate phase are not confined to a plane. A tilt of the Br–Br bond by $16 \pm 4^\circ$ had been reported in desorbed graphite bromine based on EXAFS results (Feldman *et al.*, 1986).

PHASE α

Phase α refers to the high-temperature incommensurate phase (Bardhan *et al.*, 1980). As in phase γ, the incommensurate direction of phase α is the a^*-direction (Kortan *et al.*, 1982; Erbil *et al.*, 1983a; Erbil *et al.*, 1983b), but phase α is not as incommensurate as phase γ (Figure 8).

Phase α was shown in Stage 4 to be a stripe domain phase of the Frank and van der Merwe type, with a $4\pi/7$ phase shift over a domain wall and a domain-wall width of less than one unit cell (Erbil *et al.*, 1983a; Erbil *et al.*, 1983b). The commensurate–incommensurate temperature is 342.20 ± 0.05 K. The incommensurability as a function of reduced temperature exhibits a power law with an exponent of 0.50 ± 0.02; in agreement with the prediction of Pokrovsky and Talapov (1979, 1980) for a one-dimensional commensurate–incommensurate transition in a two-dimensional lattice. This power-law fit starts deviating from the experimental points around 348 K and the incommensurability reaches its saturation at 355 K. At saturation, the domain walls are separated by about 130 Å, which is approximately 7.5 unit cells. The power-law behavior of five harmonics ($\mathbf{G}$) of the mass-density wave has been demonstrated, confirming the scaling of the structure factor with G^2 (Mochrie, Kortan, Birgenau and Horn, 1984).

The intensities of the superlattice peaks show a discontinuous drop upon heating at the commensurate–incommensurate transition temperature (Bardhan *et al.*, 1980; Bardhan, 1982; Erbil *et al.*, 1983b). The intensity discontinuity is explained by a step-function domain wall (Erbil *et al.*, 1983b).

At temperatures very close to the commensurate–incommensurate transition temperature, the incommensurate peak coexists with the commensurate peak. The halfwidth of the coexisting region is 0.2–0.4 K. This is ascribed to a slight distribution of chemical potentials for the domain walls. The transition is a solid–solid transition which is completely reversible and there is no observable hysteresis. (Erbil *et al.*, 1983b).

Ghosh and Chung (1983c) have observed the β–α (commensurate–incommensurate) transition reversibly in stage 2 (Type B) at 332 K, in stage 2 (Type A) at 333 K, in stage 3 at 337 K, and in stage 4 at 342 K (also Kortan *et al.*, 1982; Erbil *et al.*, 1983a; Erbil *et al.*, 1983b) and in Type C at 350 K (also Bardhan, 1982). Thus, the β–α transition temperature appears to increase with increasing stage number. This dependence is rather surprising because it is difficult to visualize how intercalate layers at least two carbon layers apart and uncorrelated along the *c*-direction would interact with each other in influencing the transition temperature. On the contrary, the transition temperature is expected to depend on the in-plane intercalate concentration and the domain size.

Disordering was observed upon completion of the β–α transition, so that it is an order–disorder transition involving the change of an ordered commensurate phase to a disordered incommensurate phase (Ghosh and Chung, 1983c; Erbil, Dresselhaus and Dresselhaus, 1982). In other words, the disordering involved incommensuration.

Upon heating, phase α undergoes a continuous melting transition; the x-ray diffraction intensity profiles evolve continuously from a power-law to a Lorentzian form (Bardhan *et al.*, 1980; Erbil *et al.*, 1983a; Erbil *et al.*, 1983b; Erbil *et al.*, 1982; Chung, Dresselhaus and Dresselhaus, 1977; Bardhan and Chung, 1981). The critical exponent β for the melting is 0.32 (Bardhan *et al.*, 1980; Bardhan, 1982). In the fluid phase, substantial order is maintained in the *b*-direction; that is, the fluid is actually a two-dimensional analog of a three-dimensional smectic liquid crystal (Erbil *et al.*, 1983b). The change from a two-dimensional solid phase to an anisotropic liquid phase (Phase L_1)

occurs at 373.41 ± 0.10 K (Erbil *et al.*, 1983a, 1983b). The anisotropy probably stems from the correlation between the parallel polybromide chains (Ghosh and Chung, 1983b, 1983c). Phase L_1 persists up to at least 374.0 K (Erbil *et al.*, 1983a, 1983b). Upon further heating it might transform to an isotropic liquid phase (phase L_2).

Differential scanning calorimetry (DSC) revealed that the melting transition involves two steps. The first step gave a DSC peak at 373.0 K (enthalpy change $= 178$ cal mole^{-1} Br_2); the second step gave a peak at 375.5 K (enthalpy change $= 26$ cal mole^{-1} Br_2) (Culik and Chung, 1985). There are at least two possible structural sources for the doublet. One is associated with the $\alpha \rightarrow L_1$ and $L_1 \rightarrow L_2$ transitions; another is associated with the multiphase in-plane structure in the material (Ghosh and Chung, 1983e).

PHASE α'

Phase α' refers to the low-temperature incommensurate phase which is almost identical to phase α except for a difference in the bromine atom density in the domain walls (Kortan *et al.*, 1986). Both phase α' and phase α are stripe-domain phases with a $4\pi/7$ phase shift at the domain walls. Phase α' had been observed by x-ray diffraction upon cooling phase β (stage 4) to 277 K. The transition of phase β to phase α' was sluggish, with the transformation still incomplete after 24 hr. No interlayer structural change accompanied the transition, which was first-order, with large hysteresis.

PHASE δ

Phase δ refers to the phase exhibiting the in-plane diffraction pattern shown in Figure 9(b) (Moret, Comes *et al.*, 1983). The phase was observed by x-ray diffraction upon cooling phase γ below 297 K (Moret, Comes, *et al.*, 1983) or 296 K (Aberkane *et al.*, 1985). Differential scanning calorimetry revealed an endothermic peak at 297 K during heating (Bardhan *et al.*, 1980; Culik *et al.*, 1979). Upon cooling, an exothermic peak was observed at 286 K (Bardhan *et al.*, 1980; Culik *et al.*, 1979). X-ray diffraction showed that the δ-γ transition is an

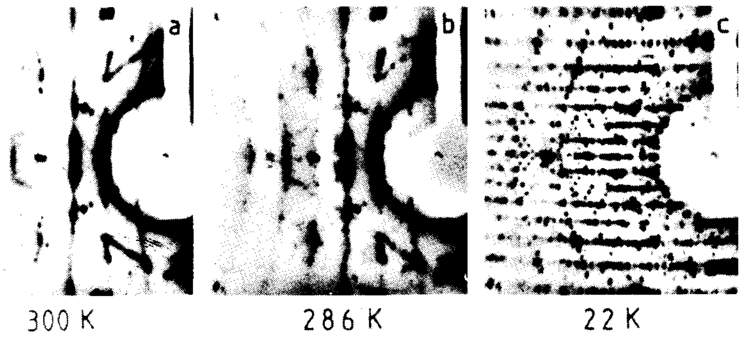

FIGURE 9 Monochromatic Laue photographs of C_8Br; $\hat{c}$ parallel to the beam. (After Moret, Rousseaux, Furdin and Herold, 1983).

interlayer order–order transition which does not affect the in-plane incommensurate structure (Aberkane *et al.*, 1985).

PHASE ε

Phase ε refers to the phase exhibiting the in-plane diffraction pattern shown in Figure 9(c) (Moret, Rousseaux, Furdin and Herold, 1983). The phase was observed by x-ray diffraction upon cooling Phase δ below 277 K (Moret, Comes, *et al.*, 1983; Aberkane *et al.*, 1985; Aberkane *et al.*, 1986). Differential scanning calorimetry revealed an endothermic peak at 277 K during heating for stage 2 only (Bardhan *et al.*, 1980; Culik *et al.*, 1979, 1984). A corresponding exothermic peak at or below the transition temperature was not observed upon cooling (Bardhan *et al.*, 1980; Culik *et al.*, 1979). X-ray diffraction revealed that the ε–δ transition was first-order, occurring at 278 K upon heating and 237 K upon cooling (Aberkane *et al.*, 1985). These observations imply that the transition during cooling is much slower than the corresponding transition upon heating. Furthermore, the enthalpy change of the ε–δ transition upon heating was sensitive to the amount of the time spent equilibrating the sample at a temperature below the transition temperature (Culik *et al.*, 1984). This sensitivity to equilibration time and temperature was not observed for the 374 K melting transition in the same material, indicating that the kinetics of the ε-δ transition are much slower than that of the melting transition.

X-ray diffraction showed that the ε-δ transition is an interlayer disorder-order transition as well as an intralayer commensurate-incommensurate transition (Aberkane *et al.*, 1985). In other words, the ε phase is commensurate and has no interlayer correlation (i.e., two-dimensional). The commensurate unit cell of ε corresponds to $\mathbf{a} = 10\,(2\mathbf{a}_g + \mathbf{b}_g)$, $\mathbf{b} = 7\,\mathbf{b}_g$, and contains 70 Br atoms (Aberkane *et al.*, 1986). The sluggishness of the δ-ε transition upon cooling is consistent with the fact that disordering occurs in this transition upon cooling. The interlayer character of this transition explains why this transition was only observed in stage 2.

The calorimetry observation of the ε-δ transition was made in Type C (Bardhan *et al.*, 1980; Culik *et al.*, 1979) while the x-ray diffraction observation was made in Type B (Moret *et al.*, 1983; Aberkane *et al.*, 1985).

Although both the ε-δ transition and the α'-β transition occur at 277 K, they are different transitions. The former is a commensurate-incommensurate transition upon heating, with the development of interlayer correlations, whereas the latter is an incommensurate-commensurate transition upon heating, with no change in the interlayer structure. The former was observed in stage 2 whereas the latter was observed in stage 4. However, both transitions are very sluggish.

PHASE η

Phase η refers to the phase exhibiting the diffraction pattern shown in Figure 5 of Bardhan *et al.*, (1980). It was observed by x-ray diffraction upon cooling Type C below 226 K. The transition corresponds to the change of streaks to spots in the electron diffraction pattern on cooling (Eeles *et al.*, 1965; Chung *et al.*, 1977) and it does not give rise to any calorimetry peak (Bardhan *et al.*, 1980). As phases γ, δ and ε were not observed in Type C by diffraction, one cannot rule out the possibility that the transition of phase β involving numerous sharp diffraction spots upon cooling stage 2 (Type A) between 240 and 230 K (Moret, Rousseaux, Furdin and Herold, 1983) is probably the same as the transition to phase η observed in Type C at 226 K (Bardhan *et al.*, 1980). This equivalence was assumed in Table I for the sake of simplicity. Moret, Rousseaux, Furdin and Herold (1983) suggested that the phase below 230 K was probably commensurate, with $\mathbf{a} = 7\,\mathbf{a}_g$, $\mathbf{b} = 6\,\mathbf{a}_g + 2\,\mathbf{b}_g$. They further noted that the transition was very slow.

DISCUSSION

This paper summarizes the current status of the subject of the structure and phase transitions of graphite-bromine. This current status is represented mostly by papers published since 1977, when a phase transition was first observed in graphite-bromine (Chung *et al.*, 1977). However, much credit should be given to the early work of Eeles and Turnbull (1965) who revealed the quasi-two dimensional nature of the bromine layers, indexed the twinned in-plane diffraction pattern using a large orthorhombic unit cell ($a = 8.5$ Å, $b = 34.5$ Å), and devised a structure exhibiting a stoichiometry of C_7Br.

The importance of synchrotron x-rays in studying graphite-bromine has been demonstrated by comparing the data on phase β obtained with sealed-tube x-rays (Ghosh and Chung, 1983b), rotating anode x-rays (Erbil *et al.*, 1983a, 1983b) and synchrotron x-rays (Ghosh and Chung, 1983b). Sealed-tube x-rays or rotating-anode x-rays yielded 9 unique hk superlattice reflections, whereas synchrotron x-rays yielded 18 unique hk superlattice reflections. The FWHM of the 3,0 superlattice peak was 0.03 Å^{-1} with synchrotron x-rays, compared with 0.18 Å^{-1} with fine-focus MoKα radiation (Ghosh and Chung, 1983b). With synchrotron x-rays, the improvement in the signal-to-noise ratio for the strong superlattice reflections was about an order of magnitude over the standard 1 kW fine-focus tube set-up.

A Br–Br distance of 2.36 ± 0.1 Å had been derived from EXAFS results on Type C graphite-bromine (Feldman *et al.*, 1984; Feldman *et al.*, 1983; Feldman *et al.*, 1986). A Br–Br distance of 2.34 Å had been derived from EXAFS results on graphite-bromine ranging from 0.27 mol % Br_2 to approximately stage 3 (Heald and Stern, 1978, 1980). However, the derivation necessitated making simplifying assumptions about the chemistry of the bromine intercalate.

Upon heating, Phase L vaporizes at 443 ± 20 K, as evident by exfoliation (Anderson and Chung, 1983a, 1984). The crystal structural (in-plane) and dimensional (c-axis) reversibility of vaporization (exfoliation), as observed in single-crystal graphite and highly-oriented pyrolytic graphite (HOPG), indicates that exfoliation is indeed a phase transition. That exfoliation involves vaporization and the subsequent collapse on cooling involves condensation is a well-accepted notion discussed by a number of authors (Anderson and Chung, 1983a, 1984; Martin and Brocklehurst, 1964; Aoki, Hirai and Yajima, 1971; Mazieres, Colin, Jegoudez and Setton, 1975; Olsen, Seeman and Scott, 1970) and recently confirmed by measurement of the pressure and volume changes at constant temperatures during exfoliation (Chung, to be published).

The temperature ranges for various stages to be stable depend on the bromine vapor pressure. This information is contained in the pressure vs. $1/T$ equilibrium diagram, as shown in Figure 2 of Anderson and Chung (1983b). The higher is the bromine vapor pressure, the higher is the upper limit of each temperature range. Thus, at the saturated bromine vapor pressure, the upper limit corresponds to the maximum temperature for stability of the given stage. These maximum temperatures are ~ 343, ~ 383, ~ 423 and ~ 523 K for stages 2, 3, 4, and 100, respectively. The value for stage 100 was calculated by using a model of intercalation, whereas the values for stages 2–4 were obtained from the experimental pressure vs $1/T$ equilibrium diagram (Anderson and Chung, 1983b). A complete phase diagram which distinguishes between phases with different in-plane structures in addition to those with different stages is not yet available.

Although much progress has recently been made in the structure and phase transitions of graphite-bromine at or above room temperature, many questions remain, particularly concerning the behavior below room temperature. The incommensurate phases are of much fundamental physical interest, but a complete structure determination of each of these phases remains to be performed. A structural elucidation of these and other phases discussed is important for understanding the mechanisms, energetics and kinetics of the phase transitions.

As a result of the determination of the two-dimensional structure of the commensurate phase (phase β), the successful use of domain-wall models to elucidate the room-temperature incommensurate phase (phase γ) (Ghosh and Chung, 1983d) and the high-temperature incommensurate phase (phase α) (Erbil *et al.*, 1983a, 1983b), and the observation of incommensurate-commensurate (γ–β) (Ghosh and Chung, 1983c, 1983d) and commensurate-incommensurate (β–α and ε–δ) (Bardhan *et al.*, 1980; Kortan *et al.*, 1982; Aberkane *et al.*, 1985; Erbil *et al.*, 1983a, 1983b) transitions, graphite-bromine has become an attractive system for the investigation of two-dimensional crystal structures (with implications on surface studies), structural relationships between commensurate and incommensurate phases, and a variety of phase transitions.

References

Aberkane F., R. Moret, R. Comes, G. Furdin and A. Herold (1985). Low temperature structural phase transitions in graphite-bromine intercalation compounds. *Abstracts, Int. Symp. on Graphite Intercalation Compounds*, Tsukuba, Japan, May, 1985, p. 3; oral presentation of paper.

Aberkane F., F. Rousseaux, E. J. Samuelson and R. Moret (1986). Structure and phase transitions of some molecular acceptor graphite intercalation compounds. *Annales de Physique*, to be published.

Al-Jishi R. and G. Dresselhaus (1983). Lattice dynamical model for graphite bromine intercalation compounds. *Mat. Res. Soc. Symp. Proc.*, **20**, pp. 301–6. Elsevier.

Anderson S. H. and D. D. L. Chung (1983a). Exfoliation of single crystal graphite and graphite fibers intercalated with halogens. *Synth. Met.*, **8**, 343.

Anderson S. H. and D. D. L. Chung (1983b). Thermodynamics of intercalation of bromine in graphite. *Mat. Res. Soc. Symp. Proc.*, **20**, pp. 271–6, Elsevier.

Anderson S. H. and D. D. L. Chung (1984). Exfoliation of intercalated graphite. *Carbon*, **22**, 253.

Aoki A., T. Hirai and S. Yajima (1971). Preparation and thermal expansion of pyrolytic graphite-bromine residual compounds. *J. Mat. Sci.*, **6**, 140.

Bardan K. K. (1982). Commensurate–incommensurate transition and disordering in dilute graphite-bromine. *Solid State Comm.*, **44**, 583.

Bardhan K. K. and D. D. L. Chung (1981). In-plane melting transitions in graphite-halogens. *Ext. Abstr. Prog.-Bien. Conf. Carbon*, **15**, pp. 113–4.

Bardhan K. K., J. C. Wu and D. D. L. Chung (1980). Phase transitions in graphite-halogens. *Synth. Met.*, **2**, 109.

Batallan F., I. Rosenman, Ch. Simon, G. Furdin and H. J. Lauter (1981). Phonons in graphite intercalated with bromine. *J. Phys., Colloq.*, **C6** 12, 344.

Batallan F., I. Rosenman and Ch. Simon (1983). Phonons and elastic constants from neutron scattering in C_7Br. *Synth. Met.*, **7**, 361.

Batallan F., I. Rosenman, Ch. Simon, H. Lauter and G. Furdin (1983). Lattice dynamics of graphite intercalation compounds. *Physica B + C* (Amsterdam), **117B** & **118B**, 614.

Cahill J. E. and G. E. Leroi (1969). Raman spectra of solid chlorine and bromine. *J. Chem. Phys.*, **51**, 4514.

Chung D. D. L. (to be published). Intercalate vaporization in graphite intercalated with bromine carbon.

Chung D. D. L., G. Dresselhaus and M. S. Dresselhaus (1977). Intralayer crystal structure and order–disorder transformations of graphite intercalation compounds. *Mater. Sci. Eng.*, **31**, 107.

Culik J. S. and D. D. L. Chung (1979). Calorimetric study of the order–disorder transformations in graphite-halogens. *Mater. Sci. Eng.*, **37**, 213.

Culik J. S. and D. D. L. Chung (1984). Calorimetric study of the rate of the 277 K phase transition in graphite-bromine. *Carbon*, **22**, 102.

Culik J. S. and D. D. L. Chung (1985). Calorimetric evidence for two-step melting in graphite-bromine. *Carbon*, **23**, 459.

Eeles W. T. and J. A. Turnbull (1965). The crystal structure of graphite-bromine compounds. *Proc. Roy. Soc.* (London), **A283**, 179.

Eklund P. C., N. Kambe, G. Dresselhaus and M. S. Dresselhaus (1978). In-plane intercalate lattice modes in graphite-bromine using Raman spectroscopy. *Phys. Rev.*, **B18**, 7069.

Erbil A., G. Dresselhaus and M. S. Dresselhaus (1982). Raman scattering as a probe of structural phase transitions in the intercalated graphite-bromine system. *Phys. Rev.*, **B25**, 5451.

Erbil A., A. R. Kortan, R. J. Birgeneau and M. S. Dresselhaus (1983a). Commensurate-incommensurate and melting transitions in bromine-intercalated single crystal Kish graphite. *Mat. Res. Soc. Symp. Proc.*, **20**, pp. 21-26 Elsevier.

Erbil A., A. R. Kortan, R. J. Birgeneau and M. S. Dresselhaus (1983b). Intercalate structure, melting, and the commensurate-incommensurate transition in bromine-intercalated graphite. *Phys. Rev.*, **B28**, 6329.

Feldman J. L., W. T. Elam, A. C. Ehrlich, E. F. Skelton, D. D. Dominguez, S. B. Qadri, D. D. L. Chung and F. W. Lytle (1983). A comprehensive investigation of residual compounds of Br in HOPG and graphite fibers via x-ray absorption. *Proc. 3rc Int. EXAFS Conf., EXAFS and Near Edge Structure*, pp. 464-467.

Feldman J. L., E. F. Skelton, A. C. Ehrlich, D. D. Dominguez, W. T. Elam, S. B. Qadri and F. W. Lytle (1984). Anisotropy effects in the linearly polarized x-ray absorption spectrum of Br_2 intercalated graphite fibers and highly oriented pyrolytic graphite. *Solid State Commun.*, **49**, 1023.

Feldman J. L., W. T. Elam, A. C. Ehrlich, E. F. Skelton, D. D. Dominguez, D. D. L. Chung and F. W. Lytle (1986). Polarized-x-ray-absorption studies of graphite intercalated-bromine compounds. *Phys. Rev.*, **B33**, 7961.

Frank F. C. and J. H. van der Merwe (1949a). One-dimensional dislocations. I. Static theory. *Proc. Roy. Soc.* (London), **A198**, 205.

Frank F. C. and J. H. van der Merwe (1949b). One-dimensional dislocations. I. Misfitting monolayers and oriented overgrowth. *Proc. Roy. Soc.* (London), **A198**, 216.

Furdin G. (1983). Étude thermogravimetrique et dilatométrique du système pyrographite HOPG-bromine. *Synth. Met.*, **7**, 101.

Gabes, W. and H. Berding (1971). Raman spectra of phosphorous pentabromide, phosphorous heptabromide and caesium tribromide. *Recl. Trav. Chim. Pays-Bas*, **90**, 157.

Gaier J. R. and D. A. Jaworske (1985). Environmental stability of intercalated graphite fibers. NASA Technical Memorandum 87025.

Ghosh D. and D. D. L. Chung (1982). Single crystal x-ray diffraction structural determination of graphite-halogens intercalation compounds. *Bull. Am. Phys. Soc.*, **27**, 273.

Ghosh D. and D. D. L. Chung (1983a). Electron diffraction evidence of domain twinning in graphite-bromine single crystals. *Mat. Res. Bull.*, **18**, 727.

Ghosh D. and D. D. L. Chung (1983b). Two-dimensional structure of bromine intercalated graphite. *Mat. Res. Bull.*, **18**, 1179.

Ghosh D. and D. D. L. Chung (1983c). Single crystal x-ray diffraction study of the phase transitions in graphite-bromine intercalation compounds. *Mat. Res. Soc. Symp. Proc.*, **20**, 15 20, Elsevier.

Ghosh D. and D. D. L. Chung (1983d). Synchrotron x-ray diffraction study of the room temperature incommensurate phase in graphite-bromine. *J. Physique Lett.*, **44**, 1761.

Ghosh D. and D. D. L. Chung (1983e). Effect of intercalate desorption on the two-dimensional structure of graphite-bromine. *Synth. Met.*, 7, 283.

Ghosh D. and D. D. L. Chung (1985). Synchrotron x-ray diffraction study of the incommensurate graphite-bromine compound: Change in the c-axis repeat distance during the incommensurate commensurate transition. *Mater. Lett.*, 3, 161.

Ghosh D. and D. D. L. Chung (unpublished results).

Heald S. M. and E. A. Stern (1978). Extended-x-ray-absorption-fine-structure study of the Br_2-graphite system. *Phys. Rev.*, **B17**, 4069.

Heald S. M. and E. A. Stern (1980). EXAFS study of Br_2-graphite compounds. *Synth. Met.*, 2, 87.

Herzberg G. (1945). *Molecular Spectra and Molecular Structure.*, D. Van Nostrand Company, Inc., Princeton, New Jersey, New York.

Kalina D. W., J. W. Lyding, M. T. Ratajack, C. R. Kannewurf and T. J. Marks (1980). Bromine as a partial oxidant. Oxidation state and charge transport in brominated nickel and palladium bis (diphenylglyoximates). A comparison with the iodinated materials and resonance Raman structure - spectra correlation for polybromides. *J. Am. Chem. Soc.*, **102**, 7854.

Kortan A. R., A. Erbil, R. J. Birgeneau and M. S. Dresselhaus (1982). Commensurate-incommensurate transition in bromine-intercalated graphite: A model stripe-domain system. *Phys. Rev. Lett.*, **49**, 1427.

Kortan A. R., R. J. Birgeneau and M. S. Dresselhaus (1986). A new commensurate-incommensurate transition of stage-4 bromine intercalated graphite. *Bull. Am. Phys. Soc.*, **31**, 597; oral presentation.

Marti C. and P. Thorel (1977). Neutron diffraction and structure of the adsorbed phases. *J. Physique*, **C4**, 26.

Martin W. H. and J. E. Brocklehurst (1964). The thermal expansion behaviour of pyrolytic graphite-bromine residue compounds. *Carbon*, **1**, 133.

Mazieres C., G. Colin, J. Jegoudez and R. Setton (1975). Mobility of bromine in its graphite and pyrocarbon residue compounds. *Carbon*, **13**, 289.

Mochrie S. G. J., A. R. Kortan, R. J. Birgeneau and P. M. Horn (1984). Algebraic decay of successive harmonics in a model two-dimensional system. *Phys. Rev. Lett.*, **53**, 985.

Moret R., R. Comes, G. Furdin, H. Fuzellier and F. Rousseaux (1983). Single-crystal x-ray scattering study of superstructures and phase transitions in graphite-HNO_3 and graphite-Br_2 intercalation compounds. *Met. Res. Soc. Symp. Proc.*, **20**, pp. 27-32, Elsevier.

Moret R., F. Rousseaux, G. Furdin and A. Herold (1983). Single-crystal x-ray study of graphite-Br and graphite-ICl intercalation compounds. *Synth. Met.*, 7, 289.

Olsen L. C., S. E. Seeman and H. W. Scott (1970). Expanded pyrolytic graphite: Structural and transport properties. *Carbon*, **8**, 85.

Pokrovsky V. L. and A. L. Talapov (1979). Ground state, spectrum, and phase diagram of two-dimensional incommensurate crystals. *Phys. Rev. Lett.*, **42**, 65.

Pokrovskii V. L. and A. L. Talapov (1980). The theory of two-dimensional incommensurate crystals *Sov. Phys.-JETP*, **51**, 134.

Reese K. M. (1983). A burst of research on hypervalent molecules is advancing bonding theory and multiplying potential applications in industry and medicine. *Mosaic*, **14**, 2.

Rüdorff W. and E. Schulze (1954). Über Alkaligraphitverbindungen. *Z. Anorg. Chem.*, **277**, 156.

Simon Ch., F. Batallan, I. Rosenman, H. Lauter and G. Furdin (1983). Lattice dynamics in second-stage bromine-graphite intercalation compound. *Phys. Rev.*, **B27**, 5088.

Song J. J., D. D. L. Chung, P. C. Eklund and M. S. Dresselhaus (1976). Raman scattering in graphite intercalation compounds. *Solid State Commun.*, **20**, 1111.

Stephens P. W., P. Heiney, R. J. Birgeneau and P. M. Horn (1979). X-ray scattering study of the commensurate–incommensurate transition of monolayer krypton on graphite. *Phys. Rev. Lett.*, **43**, 47.